The *Plasmodium falciparum* artemisinin-resistance marker *Pf*Kelch13 showing functional equivalence to the human Keap1 protein in regulating stress response and Nrf2 binding

Parveen Nikhat
Special Centre for Molecular Medicine, Jawaharlal Nehru University, New Delhi, 110067, INDIA
parveennikhat97@gmail.com

Abstract
Malaria is caused by P. falciparum and the WHO recommends artemisinin derivatives as the frontline treatment as artemisinin-based combination therapy (ACT). However, the global emergence and spread of artemisinin resistance during the past two decades has caused a serious setback in the long-term efficacy of ACT. Mutations in the P. falciparum Kelch13 (PfKelch13) protein confer artemisinin-resistance phenotype in clinical isolates and under laboratory conditions. PfKelch13 belongs to the kelch protein family and has a broad-complex, tramtrack and bric-à-brac/poxvirus and zinc-finger (BTB/POZ) domain and a C-terminal Kelch repeat propeller (KREP) domain with six kelch repeats.

Most artemisinin resistance-causing mutations occur within the KREP domain, implying its functional importance. PfKelch13 KREP shows maximum sequence homology to the KREP domain of KLHL19 (also known as Keap1; Kelch-like ECH-associated protein 1) and is speculated as a structural homolog. This study investigates the sequence-structure homology between human Keap1 and PfKelch13 to identify comparative functional aspects in mammalian cells. We hereby report that PfKelch13 in mammalian cells interacts with mammalian Nrf2 similarly to that of Keap1. Thus, our results signify the role of PfKelch13 in artemisinin-induced oxidative stress.

Keywords: *Pf*Kelch13, Keap1, Cytoprotective genes, NQO1, HO1 and Nrf2.

Introduction

Plasmodium falciparum is the most pathogenic human malaria parasite. It infects millions globally with an estimated 228 million cases documented worldwide in 2023, leading to approximately 608,000 deaths due to malaria in 2022 and a mortality rate of 14.3 deaths per 100,000 populations at risk[33]. More than 50% of all deaths occurred in just four countries i.e. Nigeria (31%), the Democratic Republic of the Congo (12%), Niger (6%) and Tanzania (4%). Around 70% of the global malaria burden is concentrated in 11 countries: Burkina Faso, Cameroon, the Democratic Republic of Congo, Ghana, India, Mali, Mozambique, Niger, Nigeria, Uganda and Tanzania[33]. Malaria results from the ongoing propagation of *P. falciparum* in human red blood cells (RBC) and artemisinin derivatives remain the only first-line treatment available.

Artemisinin-based combination therapy (ACT) is effective against both the sexual gametocytes and various asexual stages within RBCs. Artemisinin derivatives are strong antimalarial medications that act quickly and are eliminated from the body rapidly, displaying a wide range of efficacy across the parasite's life cycle stages. They can reduce parasitemia more swiftly than any other current antimalarial drugs.

However, resistance to conventional antimalarial treatments such as chloroquine and sulfadoxine-pyrimethamine, has escalated in malaria-endemic regions since the 1990s. Today, the rise of artemisinin-resistant parasites poses a significant threat[2]. In recent years, studies have indicated decreasing susceptibility to artemisinin in multiple Southeast Asian nations including Cambodia, Thailand, Myanmar and Vietnam, with a belief that this trend is continuing[1,12]. The initial phenotype of artemisinin resistance is characterized by a slower clearance of resistant parasites compared to sensitive strains in a standard *ex vivo* 72-hour ring-survival assay (RSA)[37].

Parasite lines displaying RSA values > 1 are classified as artemisinin-resistant, while those with RSA <1 are considered sensitive[37]. The primary genetic factor attributed to artemisinin resistance is single amino-acid mutations in the *Plasmodium falciparum* Kelch13 (*Pf*Kelch13) protein, which increases the likelihood of treatment failure.

*Pf*Kelch13 is a crucial member of the Kelch protein family, akin to KLHL-type proteins containing BTB and Kelch propeller regions and is integral to ubiquitin ligase complexes[38]. This protein includes a BTB/POZ domain spanning amino acids 350-437 and a C-terminal kelch repeat propeller (KREP) domain composed of six kelch motifs located between amino acids 443 and 726 (Figure 1A).

These domains promote protein-protein interactions. Nearly all mutations linked to artemisinin resistance, particularly the significant C580Y mutation, are found in the propeller domain, highlighting its functional importance[10]. The evolutionarily conserved kelch motif proteins are present across several species[25,29].

In humans, there are 42 KLHL-type proteins[10,38]. Among them, KLHL19, also referred to as Keap1 (Kelch-like ECH-associated protein1), plays a key role. Keap1 is a multi-domain protein that plays a vital role in regulating the transcription factor Nrf2 [Nuclear factor (erythroid-derived 2 -like 2)] which is involved in the production of various cytoprotective enzymes including NAD(P)H: quinone acceptor oxidoreductase 1 (NQO1), glutamate cysteine ligase (GCL) and glutathione S-transferases (GSTs), Heme Oxygenase 1 (HO1) in response to oxidative and electrophilic stress[5,23,29].

Keap1 has five distinct domains: the N-terminal region (NTR), the BTB domain, the intervening region (IVR) or BACK domain, double glycine repeats (DGR) or β-propeller domain and the C-terminal region containing kelch repeats (Figure 1B). The β-propeller and C-terminal regions together form Keap1-DC. Due to both sequence and structural similarities, *Pf*Kelch13 is regarded as a homologue of human Keap1.

Therefore, understanding Keap1 could provide insights into the functions of *Pf*Kelch13. Keap1 serves as a substrate adaptor protein for a Cul3-dependent ubiquitin ligase complex[7,18-20,34,35,41,40]. Excessive production of reactive oxygen species leads to oxidative stress in cells, contributing to various pathological conditions, including oxidative and xenobiotic stress. The Keap1-Nrf2 pathway allows cells to handle these stresses. Nrf2 interacts with Keap1 through the ETGE and DLG motifs of its Neh2 domain using a hinge-and-latch mechanism[8,15,16,24]. The ETGE motif has a stronger binding affinity to Keap1-DC compared to the DLG motif. The central core and surrounding loops of the β-propeller form a binding cavity, featuring numerous ionic residues exposed to the solvent and hydrophobic residues facing the inner surface.

Key conserved residues such as glycine, tyrosine and tryptophan are crucial for the repressive activity of the kelch domain; mutations in these residues impair this repressive role[8,28]. According to one model of the Keap1-Nrf2 antioxidant pathway, Keap1 binds to a specific level of Nrf2, maintaining low Nrf2 levels in the cytoplasm under normal conditions. When oxidative stress occurs, certain cysteine residues in Keap1 undergo modifications, releasing bound Nrf2[8]. The liberated Nrf2 moves to the nucleus, where it pairs with other transcription factors to bind to the antioxidant response element (ARE) region of phase II enzyme genes. This activation, aided by additional co-transcription factors, results in the transcription of cytoprotective genes like *nqo1, gsts, ho1 and gcl*, thereby helping to alleviate cellular oxidative stress[8,15]**.**

Based on the high sequence identity between *Pf*Kelch13 and Keap1 (Figure 3), *Pf*Kelch13 is considered a structural homolog of human Keap1. However, the functional similarity between *Pf*Kelch13 and Keap1 has not yet been explored. While the crucial role of *Pf*Kelch13 in artemisinin resistance is known, its functions in *Plasmodium* remain unclear. Our findings reveal sequence-structure homology between human Keap1 and *Pf*Kelch13 and demonstrate that both respond similarly to oxidative stress conditions, as indicated by the increased levels of cytoprotective genes during stress. Additionally, we discovered that critical functional features of Keap1 in Nrf2 binding are also present in *Pf*Kelch13.

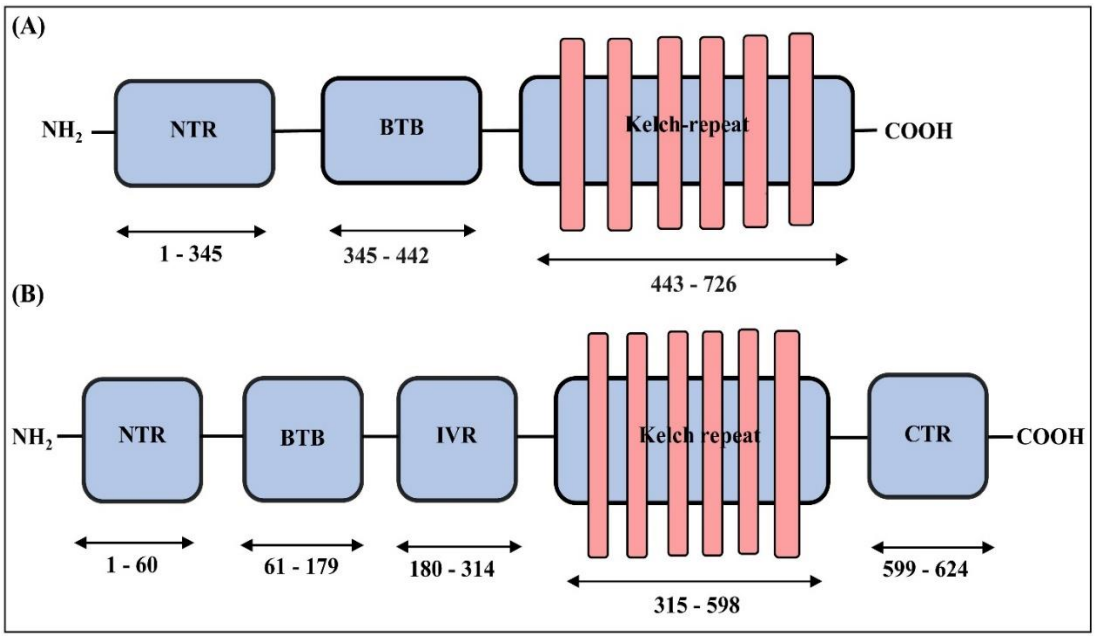

Figure 1: Schematic representations for the domain architecture of *Pf*Kelch13 and KEAP1. (A) Schematic representation of the structure of *Pf*Kelch13 (*Plasmodium falciparum*) showing the N-terminus region (NTR), broad complex, tramtrack and bric-à-brac (BTB) and kelch-repeat regions. (B) Schematic representation of the structure of Keap1 (*Homo Sapiens*) showing the NTR, BTB, intervening region (IVR), kelch-repeat region and the C-terminus region (CTR). The span of amino acids for each domain is indicated for both A and B

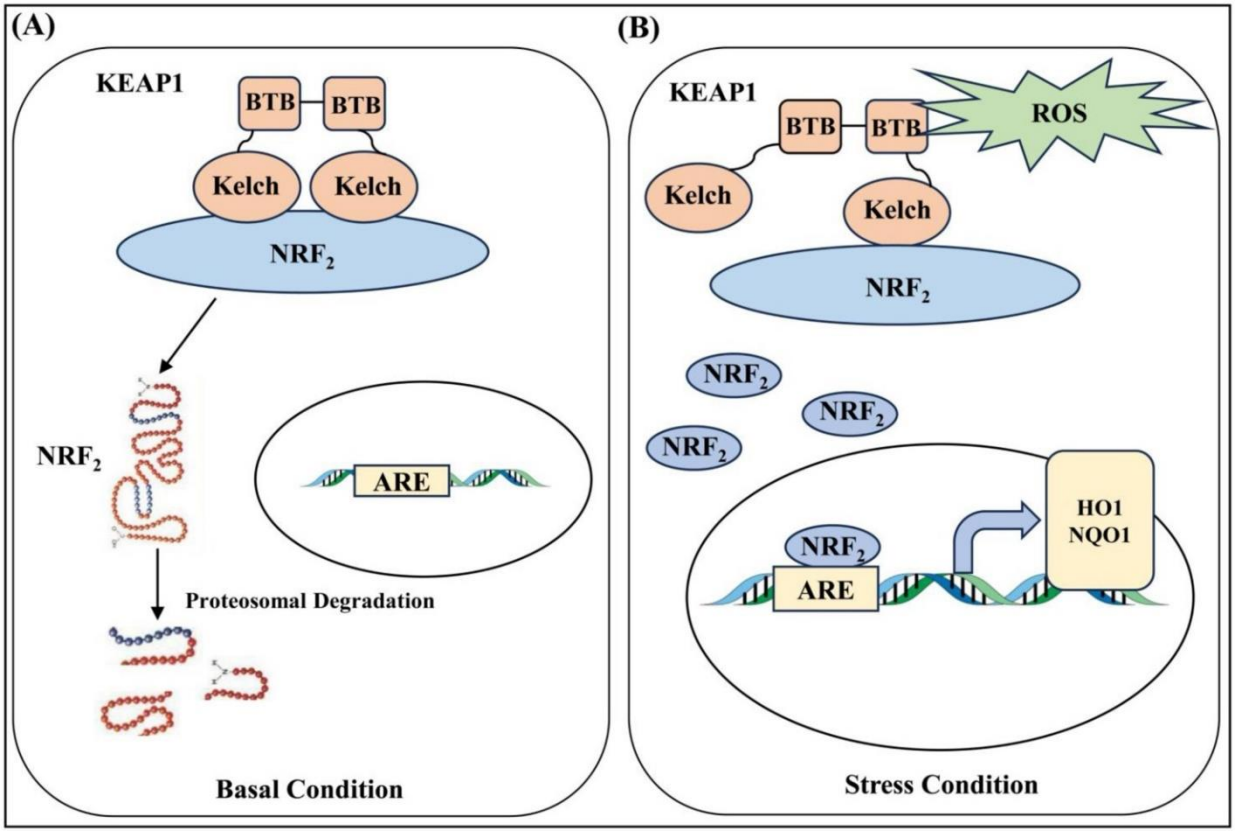

Figure 2: Schematic representation of Keap1-Nrf2 interactions under homeostatic and stress conditions. Cartoon representation of the function of Keap1. (A) During basal condition (normal), Nrf2 remain bound to Keap1 and undergoes proteasomal degradation. (B) During stress conditions, Nrf2 is released from Keap1 and translocates to the nucleus, where it activates the expression of genes like HO1 and NQO1 encoding antioxidant enzymes

Material and Methods

Reagents, chemicals and plasmid constructs: All reagents and chemicals used in this study were of analytical grade or higher and were purchased from various sources. Some of the examples of the reagent with their sources and catalogue numbers are DMEM powder (Gibco Cat. No.12100046), Opti-MEM (Gibco Cat. No.31985062), Trized RNA Extraction reagent (Edna BioLabs Cat. No.TRI-100), Helix Cript Easy cDNA kit (Cat.no. ECDNA 10-S), Fetal Bovine Serum (FBS) (Gibco Cat. No.10270106), G418 (HIMEDIA Cat. No. TC025-1G), Lipofectamine 3000 (Thermo Invitrogen Cat. No. L3000001), Protein A agarose beads (Iba life sciences Cat. No.6-2010-001), 0.5% Trypsin-EDTA (10x) and No phenol red (Gibco Cat. No. 15400054). Plasmid constructs used for this study were generated in the laboratory earlier using molecular biology grade reagents and verified by Sanger sequencing. The *Pfkelch13* gene was amplified from *P. falciparum* 3D7 genomic DNA and cloned into the pAc-GFP1-C1 plasmid.

Cell culture and preparation of cell extracts: MDA-MB, HCT-116, A549, HeLa and HepG2 cells (CRM-HTB-26, CCL-3487, CRM-CCL-185, CRM-CCL-2, HB-8065 were cultured in Dulbecco's modified eagle medium (DMEM, Gibco). DMEM from culture medium was supplemented with 10% FBS and 1% penicillin/streptomycin. Cell lines were cultured in the presence of 5% CO_2 at 37 °C. First, cells are trypsinized using 0.5% Trypsin-EDTA, 10x (Gibco) solution and pellet down further, the lysis has been done using RIPA buffer (Gibco). Cells were in RIPA (Radio-Immunoprecipitation Assay) buffer for 30 minutes in ice and further used to keep in rotation for 2 hours at 4 °C so that complete lysis of the cells takes place. Soluble extract was separated from insoluble debris after centrifugation at 10,000 rpm for 30 mins at 4 °C.

Transfection and generation of stables in A549 cell lines: Transfection of full-length *Pf*Kelch13-GFP in A549 cells was carried out using Lipofectamine 3000 reagent (Invitrogen Thermo Fischer). The manufacturer standard procedure for transfection was followed. A549 cells were seeded 24 hours before the transfection to get 80% - 90% confluency at the time of transfection. One hour before the transfection, the medium was replaced with DMEM /OPTI-MEM only. Lipofectamine 3000 reagent was added to 50 µl of DMEM/OPTI-MEM (for 24 well plate) and 250-300 ng of DNA was added to 50 µl DMEM/OPTI-MEM (24 well plate). Both the solutions were kept for 5 minutes at room temperature (RT), mixed to form a complex by incubation at RT for 30- 45 minutes (total 100 µl for each well of 24 well plate) and then added onto A549 cells.

After 12 to 16 hours, the complex was removed and replaced with a complete medium containing antibiotics. To generate

stable cell lines, transfection was done in the wild-type A549 cells grown on a 6-well plate. As previously mentioned, a complete medium was added 6 to 8 hours after transfection and maintained without antibiotics for 24 hours. Afterwards, the medium was changed to a selection medium containing G418 or gentamicin at stock conc. (50 mg/ml) and working conc. 0.4 mg/ml (HIMEDIA, TC025-1G) and the cells were cultured for 24 hours for the expression of transfected DNA. The cells in the 6 well plate were then trypsinized and seeded onto 100 mm dishes at varying dilutions (1:100, 1:250, 1:400). Small blebs represented different colonies that started to form after 2-3 weeks of incubation. By carefully isolating them with trypsin, these colonies were then carefully seeded into wells of a 48-well plate. Different clones were checked for GFP-tagged protein expression and localization by IFA and western blotting.

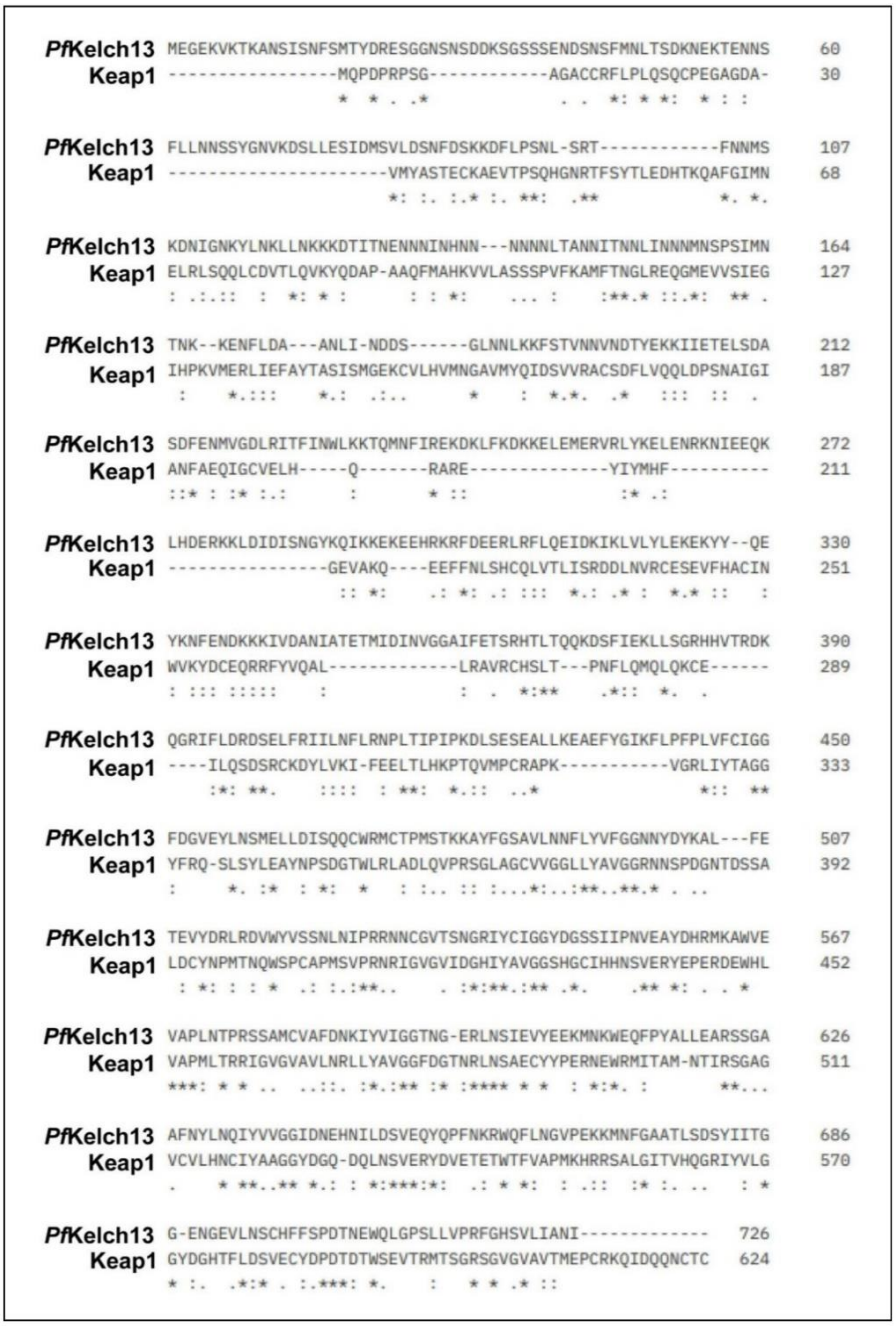

Figure 3: Sequence alignment between *Pf*Kelch13 (PF3D7_1343700) with its human ortholog Keap1. The * indicates that the residues at this position are fully conserved across all sequences in the alignment. This means that every sequence has the same amino acid or nucleotide at this position, suggesting a critical role in structure or function. Here, these amino acid lies mostly in the KREP domain region of both *Pf*Kelch13 (443-726) and Keap1 (315-598). (.) represents positions in the alignment not conserved but are similar. It indicates that the residues at the position in the aligned sequences are different but share some level of similarity, typically in their chemical properties. (:) Signifies a moderate level of conservation. Specifically, it indicates that the residues are not identical but are similar enough to be grouped, often due to having similar chemical properties

Western blotting: The preparation of whole cell lysates was one, as mentioned earlier. Protein concentration was determined using Bradford protein assay (HIMEDIA). Proteins (20 to 40 µg) were resolved by SDS-PAGE and transferred to nitrocellulose membranes. Membranes were incubated with primary antibodies overnight at 4 °C. Anti-GFP antibody (Invitrogen, Rabbit) was diluted at 1:2000 and anti-Keap1 antibody (Cloud clone, Rabbit) was diluted at 1:1500. After the overnight binding of the membrane with primary antibody, again washing of the membrane was done with PBST buffer to remove the excess of primary antibody and the further membrane has been probed with secondary Rabbit Horseradish-peroxidase conjugated antibody (BioBharati Life Sciences) for one hour with the dilution of 1:5000 and kept at room temperature for 1 hour to verify the expression of *Pf*kelch13-GFP, AcGFP and Keap1 respectively.

Immunofluorescence Assay: Cells non-transfected A549, transgenic (*Pf*Kelch13-GFP, AcGFP) and MDA-MB-231 in the exponential growth phase were digested with trypsin and re-suspended and the cell density was adjusted to 1×10^6 cells/ml with culture media. Before cell density adjustment, one glass coverslip (22 × 22 mm) was placed into each well of a 6-well dish. A total of 5 µl of cell suspension was seeded onto the glass coverslip to grow up to 30-50% confluence 24 hours later. Following incubation for the specified durations, the media were removed and cells were washed three times with ice-cold PBS. The slides of cells were fixed in fresh 4% formaldehyde for 20 min at room temperature. Subsequently, the cells were washed three times with PBS and incubated in PBS containing 1% (v/v) triton X-100 and 1% bovine serum albumin (Sigma) for 1 hour on ice to permeabilize the cells and block non-specific protein-protein interactions.

The glass coverslips were removed from the 6-well plates and subsequently incubated with 50 µl GFP (1:200) primary antibody (Invitrogen, Rabbit) in case of transgenic (*Pf*Kelch13-GFP and AcGFP) and Keap1 Primary antibody (Cloud-clone, Rabbit) in case of Keap1 expressing cell line diluted at 1:200 and placed at room temperature for 2 hours. The secondary antibodies used were FITC (ICN Biochemical Rabbit) and TRITC (ICN Biochemical Rabbit), which were used at a 1:200 dilutions for 1 hour. DAPI (Sigma) was used to stain the cell nuclei for 5 min at room temperature. Finally, the coverslips were sealed and observed under fluorescence microscopy.

Hydrogen peroxide treatment: A549 cells were grown till they were 90%-100% confluent in a CO_2 incubator. Before drug treatment, the cell monolayers were washed with PBS (phosphate-buffer saline solution) buffer and treated with hydrogen peroxide. After the treatment, cell extracts were prepared and subjected to cDNA synthesis using an easy cDNA kit (Cat. No. ECDNA 10-S) for RT-qPCR reaction to check the mRNA expression level of cytoprotective gene levels (HO1, NQO1) using an eDNA kit as per the protocol.

MTT cell viability assay: 1×10^5 cells/100 µl per well of transgenic A549 (*Pf*Kelch13-GFP and AcGFP) and non-transfected A549 cells were seeded in flat bottom 96 well plates with different concentrations of H_2O_2 (50 µM, 100 µM, 150 µM, 200 µM) to determine the dose-response relationship for cell viability. The cells were incubated for 24 hours at 37 °C. 5 mg/mL MTT dye [3-(4,5-dimethyl-2-thiazolyl)-2,5-diphenyltetrazolium bromide] stock was prepared in 1X PBS. MTT assays were performed as per the manufacturer's protocol. Briefly, after 24 hours of incubation, 10 µl of MTT dye was added from the stock 5 mg/mL and the overall working concentration of MTT dye (SRL) was 0.5 µg/µl.

Incubated at 37 °C for 4 hours or until the purple colour developed, the reaction was stopped by DMSO as a solubilization buffer and incubated at 37 °C with mild shaking to dissolve formazan crystals. Absorbance was measured at 570 nm and percentage viability was calculated. Transgenic A549 (AcGFP) cells were used as a positive control and only DMEM media were used as a negative control. MTT dye was light-sensitive, so all experimental steps were performed only in the dark. Each experiment was performed in triplicate.

RT-qPCR: Cells were seeded in 6-well plates and treated with 0 µM, 50 µM, 100 µM, 150 µM and 200 µM H_2O_2. Total RNA was extracted from cells using Trizol RNA extraction reagent. (Edna Biolabs Cat. No.TRI-100). RNA quality and quantity were measured using a NanoDrop 2000 spectrophotometer (NanoDrop Technologies; Thermo Fisher Scientific, Inc.). A total of 1 µg RNA was reverse transcribed into cDNA using the Easy cDNA synthesis kit (Cat. No. ECDNA10-S) in a final 20 µl volume reaction, according to the manufacturer's protocol. A volume of 1 µl RT reaction mixture and 9 µl qPCR mixture was mixed and SYBR Green I-based RT-qPCR analyses of human NQO1 and HO1 were performed by using the SYBR eDNA according to the manufacturer's protocol in duplicate on an ABI 7500 system (Applied Biosystems; Thermo Fisher Scientific, Inc.). All primers were designed and synthesized by Eurofins Co.

Forward primers:

HO1	5'ATGACACCAAGGACCAGAGC3'
NQO1	5'CCTTCCGGAGTAAGAAGGCAG3'
GAPDH	5'CAGGAGGCATTGCTGATGAT3'

Reverse primers:

HO1	5'GCATAAAGCCCTACAGCAACT3'
NQO1	5'TCCAGGCGTTTCTTCCATCC3'
GAPDH	5' GAAGGCTGGGGCTCATTT3'

GAPDH was used as a reference gene. The $2^{-\Delta\Delta}$C q method determined the relative quantitative levels of samples.[4]

Immunoprecipitation: A549 cells were grown to confluency in 100 mm culture plates and extracted in 500 µl

cell lysis buffer (RIPA buffer). The cell extract was passed through an 18-gauge needle (three times), then a 22-gauge needle (three times) and then incubated on ice for 30 minutes. The cell extract was centrifuged at 12000 rpm for 10 minutes at 4 °C. The supernatant was collected and added to the GFP antibody bounded Protein A agarose /Sepharose beads (IBA LifeScience) and incubated overnight on a rotor spin at 4 ºC at 6-7 rpm. The beads were pelleted the next day and washed thrice with cell lysis buffer at 4000 rpm (4 °C). After the final wash, the beads were suspended in 2x SDS gel loading dye and the samples were electrophoresed on 10% gels to identify potential protein interactions.

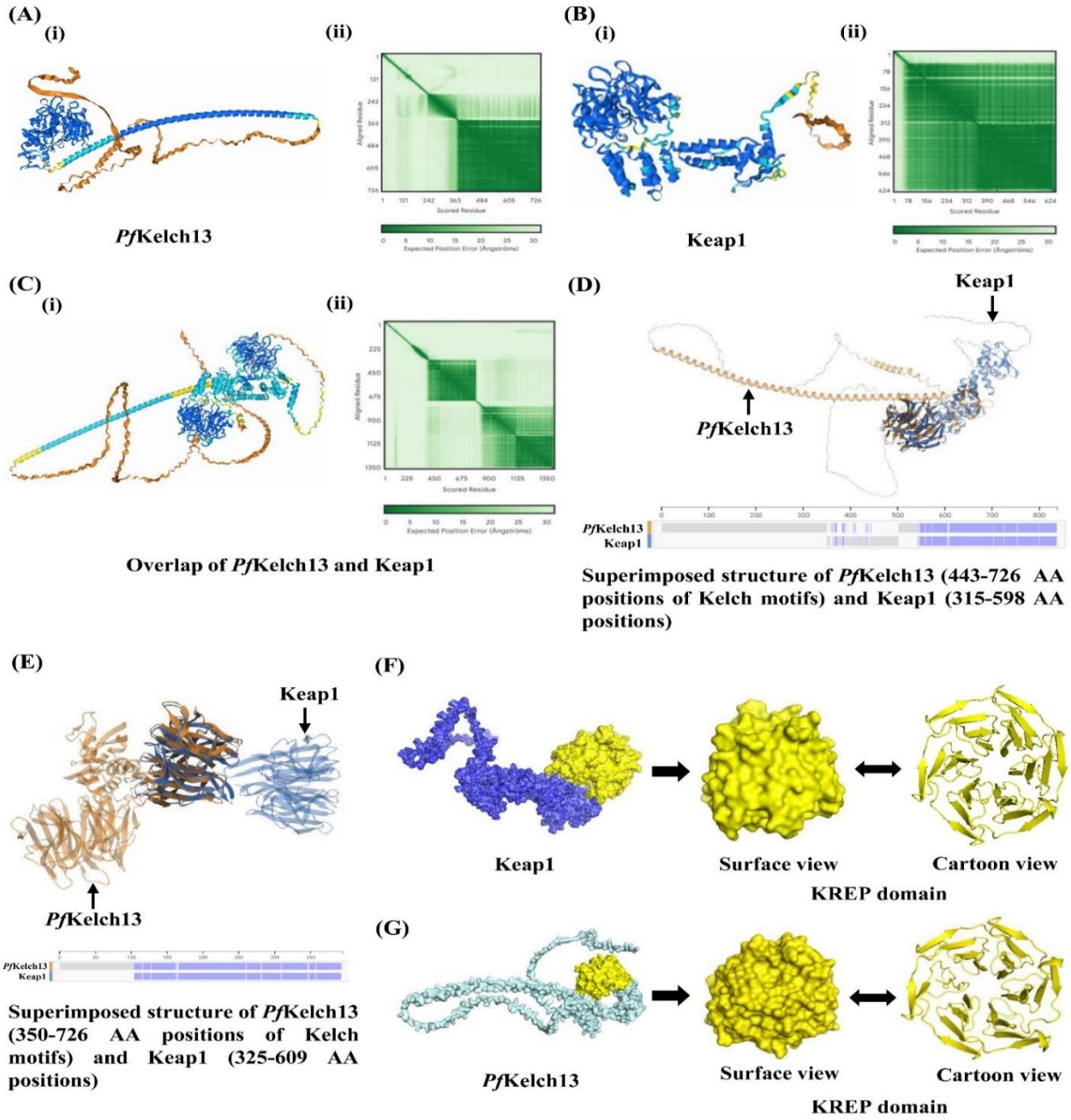

Figure 4: *In silico* structural analysis of conformational folding of *Pf*Kelch13 and Keap1 protein. (Ai): Cartoon representation of the full-length *Pf*Kelch13 structure using RCSB Pair-wise structure alignment method: TM-Align having pTm value of 0.56 (Aii): The larger green portion shows lesser error in structure prediction, which lies in KREP domain region of amino acid of *Pf*keclh13 (Bi): Cartoon representation of the full-length Keap1 structure using RCSB pair-wise structure alignment method: TM-Align having pTm value of 0.79 (Bii): The larger green portion shows lesser error in structure prediction which lies in KREP domain region of amino acid of Keap1 (C): Overlap structure of both full-length *Pf*Kelch13 and Keap1 (D): Superimposed image generated after Pair-wise structure alignment showing RMSD value 3.33 and identity 22%. (E): Sequence alignment of the *Pf*Kelch13 structure (PDB ID: 4YY8) and Keap1(PDB ID: 6FMP), Superimposed image generated after pair-wise structure alignment of both *Pf*Kelch13 structure (PDB ID: 4YY8) and Keap1(PDB ID: 6FMP), showing RMSD value 1.42 and identity 25%. (F and G): Comparison of the structure of KREP domain of both Keap1 and *Pf*Kelch13

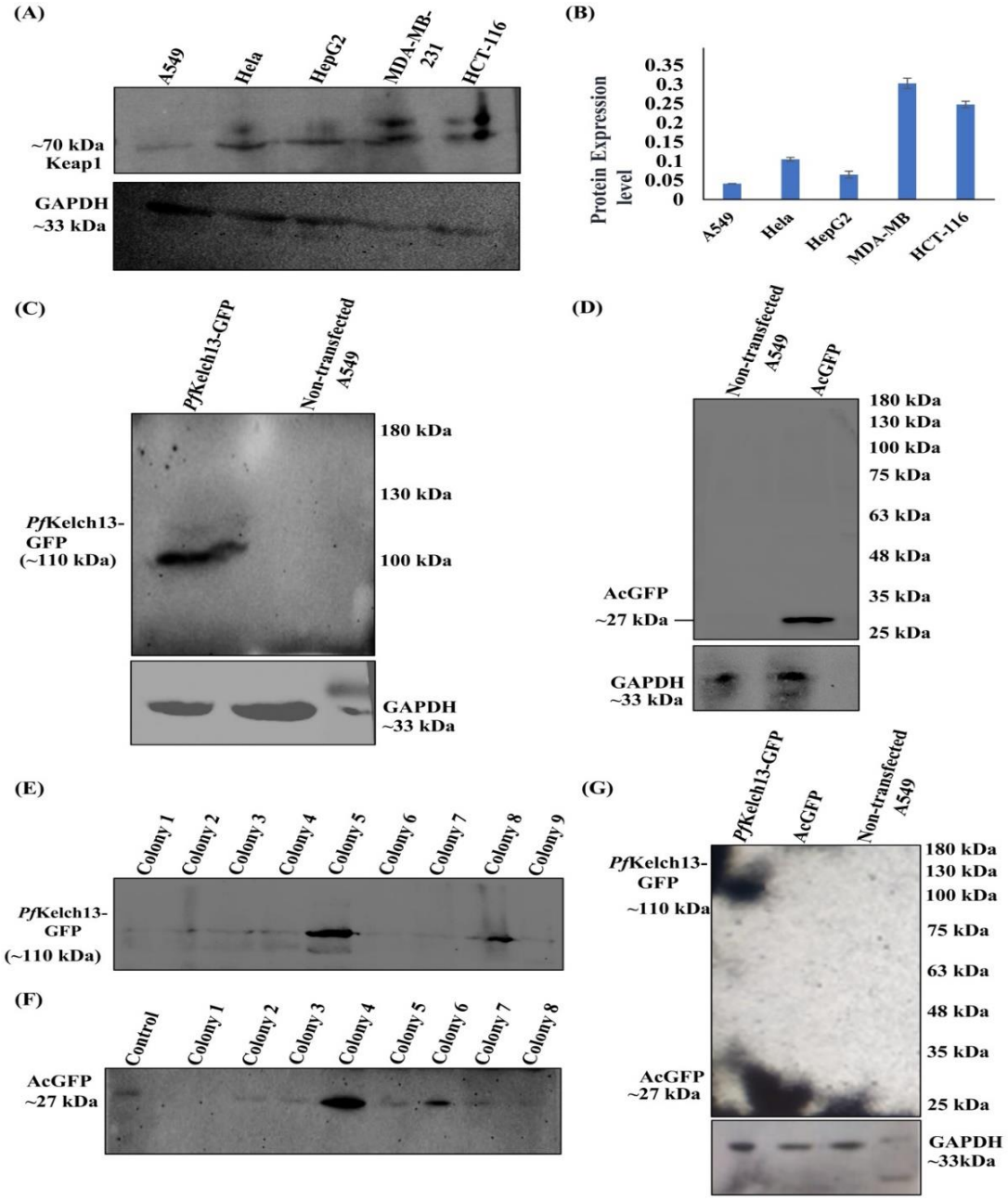

Figure 5: Validation of *Pf*Kelch13 and AcGFP expression in transgenic mammalian cells.
Western blot expression of Keap1 in different cell lines, along with recombinant *Pf*Kelch13 and AcGFP expression after transient and stable transfection in A549 cells. (A): Protein levels of Keap1 (whole-cell lysate) were evaluated by western blot. GAPDH (whole-cell lysate) served as loading controls. Based on KEAP1 protein levels, cell lines were categorized according to their high and low Keap1-expressing cell lines. (B): Ration of Protein expression level of different cell lines vs. GAPDH of (Figure 5A) using ImageJ. (C): Western blot analysis of *Pf*Kelch13-GFP expression in A549 cells (Transient transfection). Extracts of cells were prepared 24 hr post-transduction. The blot was probed with an antibody directed against GFP; non-transfected A549 cells were used as a control; GAPDH (whole-cell lysate) served as a loading control. (upper blot topmost left side band of size 110 kDa of *Pf*Kelch-GFP in transfected A549 cells) (D): Western blot analysis of AcGFP vector expression in A549 cells (Transient transfection). Extracts of cells were prepared 24 hr post-transduction. The blot was probed with an antibody directed against GFP; non-transfected A549 cells were used as a control; GAPDH (whole-cell lysate) served as a loading control and was probed with anti-GAPDH antibody (upper blot, topmost right side band of size 27 kDa of AcGFP in transfected A549 cells). (E): Western blot analysis of *Pf*Kelch13-GFP expression of different colonies formed after transfection and under continuous selection of cells in G418 antibiotic (HIMEDIA, TC025-1G) present in DMEM media (Stable transfection). (F): Western blot analysis of AcGFP expression of different colonies formed after transfection and under continuous selection of cells in G418 antibiotic present in DMEM media (Stable transfection). (G): Positive colony of *Pf*Kelch13-GFP and AcGFP is again confirmed by western blot with equal loading with GAPDH

Results

***In silico* analysis revealing structural similarities between *Pf*Kelch13 and KEAP1, especially in the KREP domains:** Many prior large-scale structure prediction efforts focused on domains, sections of the sequence that fold independently. To date, the crystal structure of the C-terminal portion of *Pf*Kelch13 covering the BTB and the KREP is available like PDB ID: 4YY8, as well as of the Keap1-peptide complex (PDB ID: 6FMP). Sequence alignment and pairwise alignment were performed using the Clustal Omega server (https://www.ebi.ac.uk/jdispatcher/msa/clustalo) and NCBI BLAST (https://blast.ncbi.nlm.nih.gov), revealing a sequence identity percentage of 27.94% and maximum identical amino acids in their KREP domain region (Figure 3).

Next, using the AlphaFold3 server (https://alphafold.ebi.ac.uk), we attempted to predict the full-length structure of both the *Pf*Kelch13 and Keap1 and superimposed them to check the structural similarity of both the predicted structures of *Pf*Kelch13 and KEAP1. We also superimposed the *Pf*Kelch13 and Keap1 structures already present in the PDB database with PDB IDs 4YY8 and 6FMP (https://doi.org/10.2210/pdb4YY8/pdb, https://doi.org/10.2210/pdb6FMP/pdb) respectively to validate our result from AlphaFold3 predicted structures superimposition. Surprisingly, the AlphaFold3 predicted full-length structure of *Pf*Kelch13 shows pTm 0.56 and Keap1 shows 0.79 denoting good accuracy of the predicted structures.

The dark blue coloured region showed maximum confidence of more than 90, which means the region shows the highest accuracy, while the light blue region shows confidence between 90 to 70, yellow shows confidence between 70 to 50 and orange shows less than 50. [Figure 4 A(i) and B(i)] In both the AlphaFold predicted Protein structures (*Pf*Kelch13 and Keap1), the dark blue region is the KREP domain region, meaning the particular region highly resembles the original structure.

Expression of KEAP1 in mammalian cells: The main objective of our study was to determine whether *Pf*Kelch13 shows functional resemblance with its human ortholog Keap1. We reasoned that *Pf*Kelch13 would regain all the functions of Keap1 when transfected in the low Keap1 expressing cell line. However, the status of Keap1 has been reported for very few common cancer cell lines[26].

Therefore, to evaluate the cell line with low Keap1 expression, we have taken cell lines known for different Keap1 levels (MDA-MB-231, HCT-116 as High Keap1 expressing cell lines; HeLa, A549 as Low Keap1 expressing cell lines and HepG2 as moderate Keap1 expressing cell lines) and cultured them under appropriate condition and further checked the Keap1 expression by western blot using anti-Keap1 antibody observed the band at 70 kDa in HCT-116, MDA-MB-231, HepG2, HeLa, A549 (Figure 5A) upper blot from the rightmost band of blot to the most left band respectively). We observed that the Keap1 expression band in A549 was very faint or almost none. GAPDH was used as a loading control and detected using an anti-GAPDH antibody at a dilution of 1:3000. (band size of 33 kDa was observed) (Figure 5A) lower blot shows GAPDH expression).

The protein expression intensity graph has been plotted to verify the equal loading by measuring the intensity of the bands observed in the western blot (Figure 5B). Our western results confirmed that Keap1 expression in the A549 is extremely low or almost absent.

Transient expression and generation of stable A549 cell line expressing *Pf*Kelch13-GFP and AcGFP: *Pf*Kelch13 (PlasmoDB ID: PF3D7_1343700) gene was cloned into the mammalian expression plasmid pAcGFP1-C1 plasmid under the control of CMV promoter (generated previously in the laboratory). The pAcGFP1-C1 plasmid with *Pf*Kelch13 was then transfected in A549 mammalian cell line, with AcGFP as an independent transfection and used as a control in our subsequent experiments. All the transient expressions are checked via western blot and live cell imaging. We observed the band of 110 kDa in recombinant *Pf*Kelch13 *(Pf*Kelch13-GFP*)* in transfected A549 cells (Figure 5 Panel C: Upper blot topmost left-side band) but not in non-transfected.

Similarly, we got the band of size 27 kDa in AcGFP transfected A549 cells (Figure 5 Panel D upper blot topmost right-side band) but not in non-transfected. We further proceed for the generation of transgenic or stable cell lines for both *Pf*Kelch13 as well as AcGFP1 by keeping transiently transfected cells under continuous selection of G418.

Clones were confirmed by western blots using anti-GFP antibody (Figure 5 Panel E colonies 5 and 8 represent positive clones for *Pf*Kelch13) (Figure 5 Panel F: Colonies 4 and 6 represent positive clones for AcGFP) and again reconfirmed one of the positive clones of both (Figure 5 Panel G upper blot right side lower band of 27 kDa show positive AcGFP clone and topmost left band of 110 kDa shows positive clone of *Pf*Kelch13). GAPDH was used as a loading control and detected using an anti-GAPDH antibody at a 1:3000 dilutions for subsequent experiments. (Figure 5 Panel C, D and G lower blot showed a band size of 33 kDa of GAPDH).

The localization profile in transgenic A549 (*Pf*Kelch13-GFP) as compared to Keap1 in MDA-MB-231 cells: To determine the cellular distribution of endogenous Keap1 protein, we performed an immunofluorescence assay (IFA) with MDA-MB 231 (High Keap1 expressing) cells using anti-Keap1 antibody. Similarly, to check the subcellular location of transgenic *Pf*Kelch13-GFP, we performed IFA using GFP antibodies.

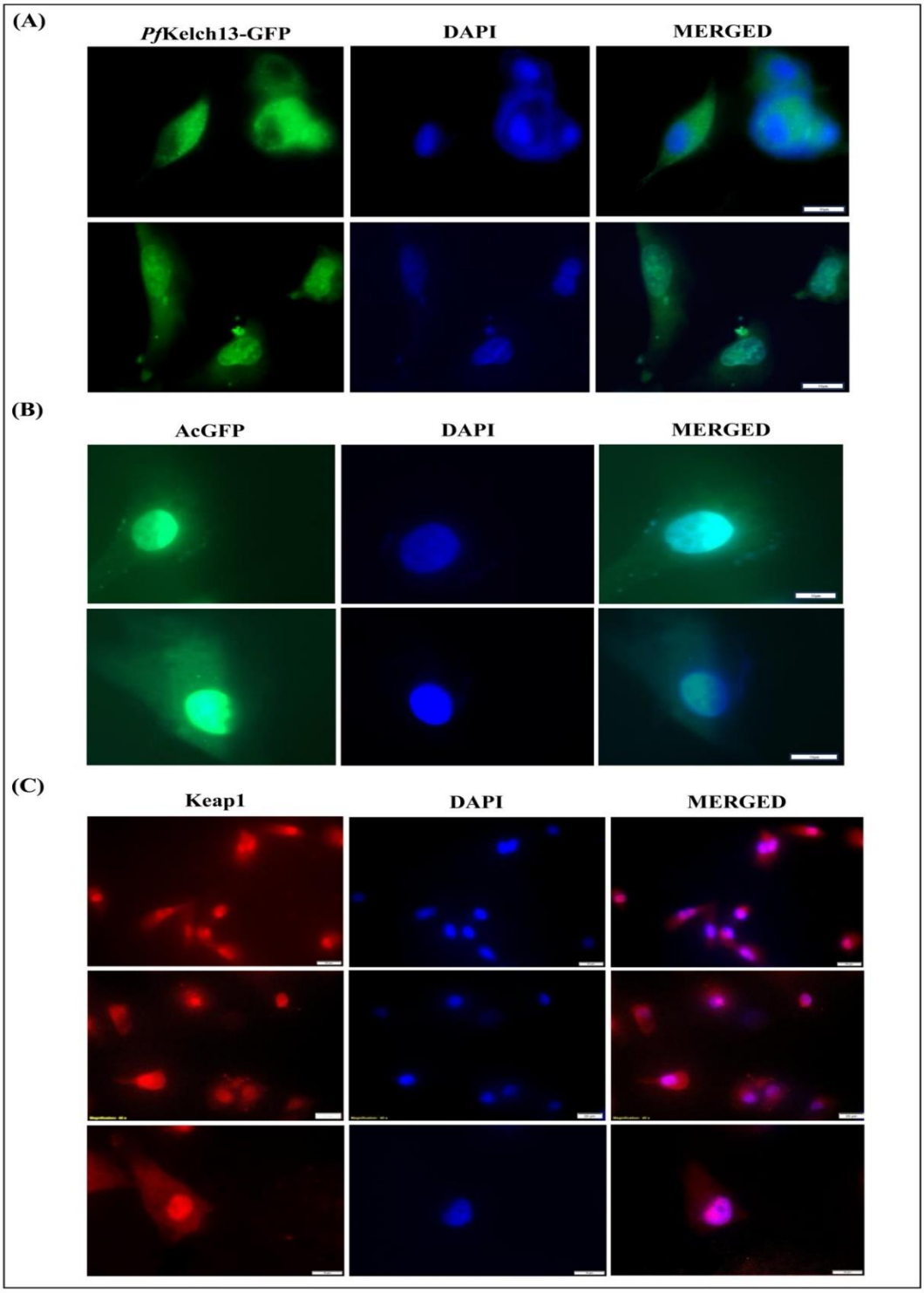

Figure 6: After transfection, the expression and localization analysis of *Pf*Kelch13 and Keap1 in A549 and MDA-MB-231 cell lines. (A): IFA images of Recombinant *Pf*Kelch13 after transfection in A549 using GFP-specific primary antibody (anti-rabbit, 1:200), followed by FITC conjugated anti-rabbit (green), secondary antibodies (1:200 dilution). DAPI staining shows nucleoid position in the cell (Hoechst 33258 was used for nucleus staining) merge overlay of *Pf*Kelch13-GFP with DAPI (Panel B: Scale bar: 10 μm) (B): IFA images revealing the localization of AcGFP using GFP-specific primary antibody (anti-rabbit, 1:200) followed by FITC conjugated anti-rabbit (green), secondary antibodies (1:200 dilution). DAPI staining shows the nucleoid position in the cell (Hoechst 33258 was used for nucleus staining); merge overlay of AcGFP with DAPI (Panel A: Scale bar: 10 μm). (C): IFA images revealing the localization of Keap1 in MDA-MB-231 using Keap1 specific primary antibody (anti-rabbit, 1:200), followed by TRITC conjugated anti-rabbit (red), secondary antibodies (1:200 dilution). DAPI staining shows nucleoid position in the cell (Hoechst 33258 was used for nucleus staining); merge overlay of KEAP1 with DAPI (Panel C Scale bar: 20 μm: lane1 and lane 2, Scale bar: 10 μm lane 3)

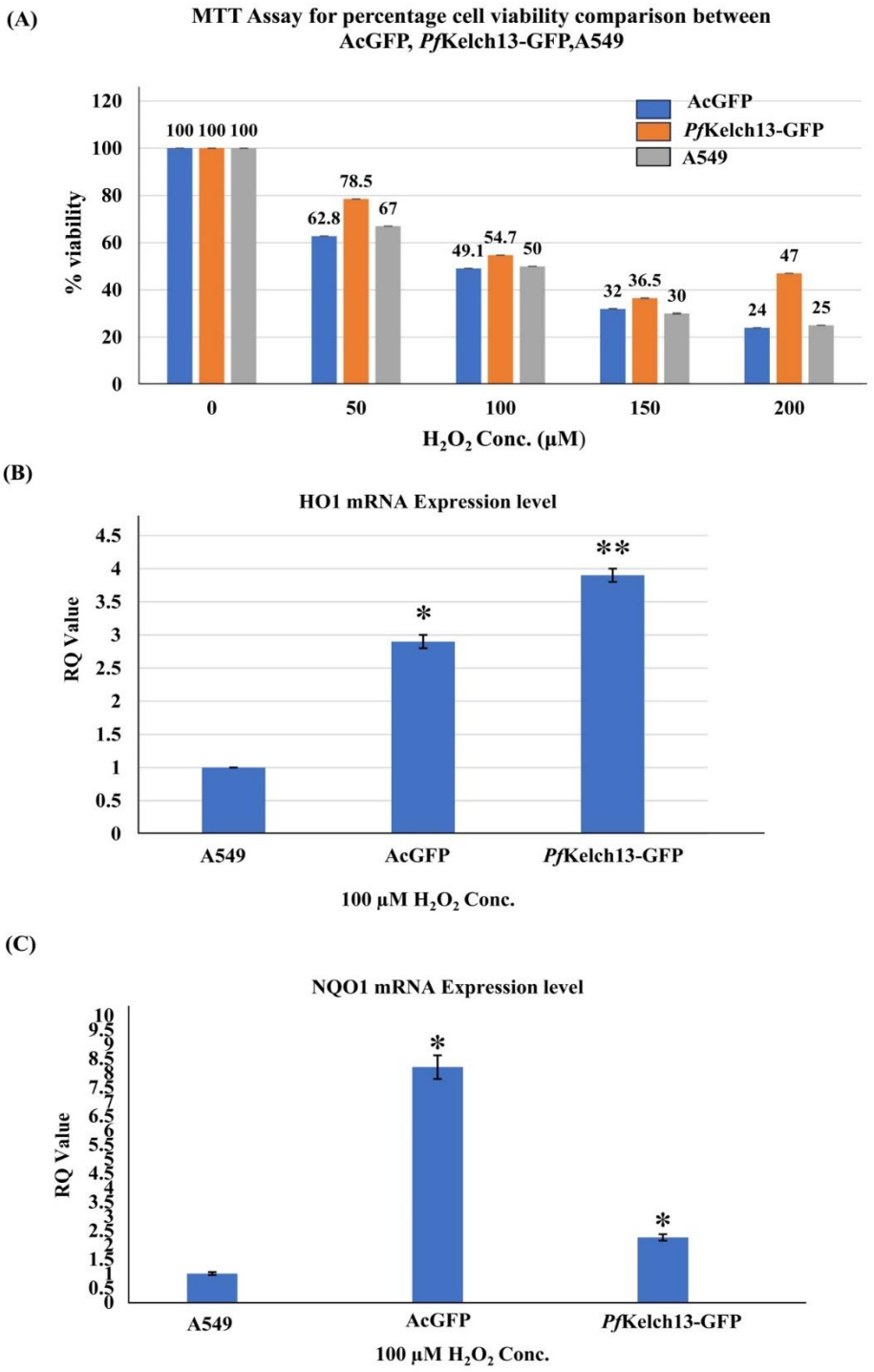

Figure 7: Effect of H_2O_2 on cell viability and cytoprotective gene expression level of transgenic A549 (*Pf*Kelch13-GFP and AcGFP) and non-transfected A549. (A): Proliferation assay: Graph of MTT assay after 24 hours shows the percentage of cell viability of A549 (non-transfected), as well as *Pf*Kelch13-GFP and AcGFP (transfected), after exposure to concentrations 50 µM, 100 µM, 150 µM, 200 µM of Hydrogen peroxide (H_2O_2) used to generate the oxidative stress condition. Positive control shows cells without exposure to any H_2O_2 used 100 per cent cell viability, while at different concentrations, there is a fall in the percentage of cell viability.

Based on the percentage cell viability of cells, 100 µM has been selected for further experiments (percentage cell viability more than 50 per cent) as the aim is to identify the concentration of H_2O_2 to produce the stress condition in cells without too much cell death. (B): HO1 mRNA levels seem to be high in comparison to non-transfected low keap1 expressing A549 cells, which indicates that during oxidative stress conditions in the presence of *Pf*Kelch13, cytoprotective genes like NQO1 and HO1 levels increase. (C): NQO1 mRNA levels for individual cell lines were measured by RT-qPCR. *p< 0.05, ** p< 0.1 for AcGFP and *Pf*Kelch13-GFP respectively, the p-value was calculated based on two paired unequal variable t-test comparing AcGFP and *Pf*Kelch13-GFP to A549

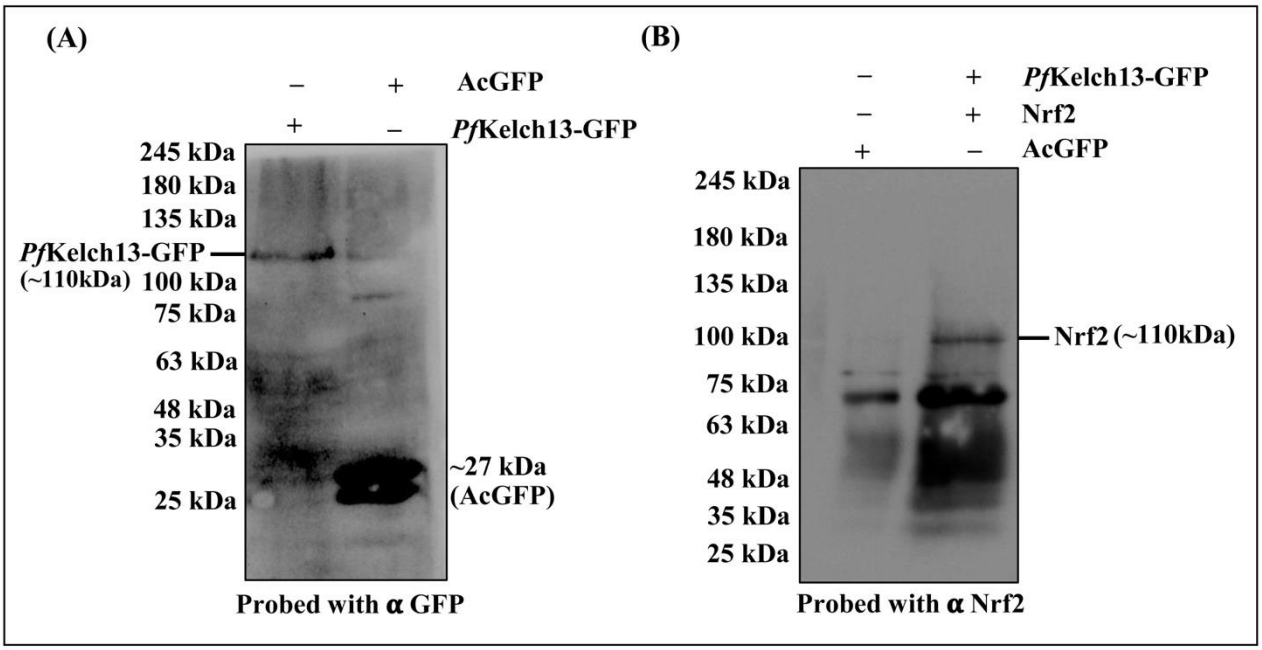

Figure 8: Western blot analysis to identify Nrf2 interaction with *Pf*Kelch13. Whole-cell lysates were prepared by lysing the cells in lysis buffer (RIPA). Transgenic AcGFP and *Pf*Kelch13-GFP will be immunoprecipitated using anti-GFP antibody, followed by protein A-conjugated agarose/Sepharose beads. The binding partners that co-immunoprecipitated from the above experiments will be identified by western blotting using anti-Nrf2, which was one of the known interacting partners of Keap1 (A): Protein expression of *Pf*Kelch13-GFP (molecular mass 110 kDa approx. Figure 8. A top most left side band of blot) and AcGFP (molecular mass of only GFP, 27 kDa approx. Figure 8. (B): An upper band on the right side of the blot). B: AcGFP was used as a negative control and *Pf*Kelch13-GFP sample lane showed Nrf2 (Mol. Wt. 110 kDa approx. Figure 8. B topmost right-side band of blot)

We further assessed if the green fluorescence profile of transgenic *Pf*Kelch13-GFP was different from the only GFP profile (in AcGFP expressing cells as a control). The results demonstrated that Keap1 localizes mainly in the perinuclear area of cytoplasm and interestingly, we found that transgenic *Pf*Kelch13-GFP localizes mainly in the perinuclear area of cytoplasm as well as the green fluorescence signal was more compact and lies within the cell with no or significantly background green fluorescence similar to localization profile of Keap1 (Figure 6A).

The only GFP localization profile from transgenic AcGFP shows that GFP localizes mainly in the nuclear region and significantly less in the area of cytoplasm also giving background green fluorescence too (Figure 6B).

Comparative growth and oxidative stress response gene expression in transgenic A549 expressing *Pf*Kelch13-GFP: To date, several studies have investigated the effects of the KEAP1- Nrf2-antioxidant response element (ARE) signaling pathway. One of the most important *in vivo* cell defense and survival mechanisms is the kelch-like ECH-associated protein 1 (KEAP1)/nuclear factor erythroid 2-related factor 2 (Nrf2) system[32].

Under oxidative stress, Nrf2 translocates into the nucleus to bind the antioxidant response element (ARE), which increases the expression of downstream antioxidative proteins like heme oxygenase 1 (HO1) and NAD(P)H quinone oxidoreductase 1 (NQO1). In the resting state, Nrf2 is retained in the cytoplasm by KEAP1.

To study the role of transgenic A549 (*Pf*Kelch13-GFP) against oxidative damage, the resistance of the cells to oxidative stresses induced by H_2O_2 was analyzed with the help of RT-qPCR by measuring the change in mRNA level of cytoprotective genes like heme oxygenase 1 (HO1) and NAD(P)H quinone oxidoreductase 1 (NQO1)[4]. We first investigated the effect of H_2O_2 on cell viability of both non-transfected A549 and transgenic A549 (*Pf*Kelch13-GFP and AcGFP). H_2O_2 has been widely accepted to cause cell death[13,30]. The MTT assay data (Figure 7A) revealed that the cell viability remarkably decreased with H_2O_2 from 50-200 µM in both the non-transfected A549 and transgenic A549 (expressing either *Pf*Kelch13-GFP or AcGFP). The results suggested that exposure to H_2O_2 resulted in a notable decrease in viability in the non-transfected A549 as well as transgenic A549 expressing AcGFP.

However, the survivability was better in transgenic A549 (*Pf*Kelch13-GFP) (Figure 7A). On dose-dependent comparison, results also indicated that the cell viability of both non-transfected A549 and transgenic A549 (*Pf*Kelch13-GFP and AcGFP) was reduced to approximately 50 per cent in cells when treated with 100 µM concentration of H_2O_2 for 24 hours. We used 24-hour exposures of 100 µM H_2O_2 for later studies based on the above results[39]. To further validate the classification of the non-transfected and

transgenic A549 (*Pf*Kelch13-GFP and AcGFP) cell lines, we measured the levels of other biomarkers of Keap1 activity, including NQO1 mRNA and HO1 mRNA levels. Thus, once the concentration was selected, both the non-transfected and transgenic A549 (*Pf*Kelch13-GFP and AcGFP) were kept under oxidative stress (100 μM H_2O_2) for about 24 hours.

RT-qPCR was performed to check the mRNA level of HO1 and NQO1 in all these cell lines. GAPDH was used as a reference gene. Relative quantitative (RQ) levels of samples were determined by the $2^{-\Delta\Delta Cq}$ method[4]. The relative quantification values of HO1 for A549, *Pf*Kelch13-GFP and AcGFP we got, were 1, 3.8 and 3.0, taking A549 as a control. The relative quantitative (RQ) values of NQO1 for A549, *Pf*Kelch13-GFP and AcGFP we got, were 1, 2.25 and 8.19. Thus, as we saw, the value of RQ of *Pf*Kelch13-GFP was approximately three times higher than non-transfected A549 in both the HO1 and NQO1 (Figures 7B and C) respectively.

Nrf2 as an interacting partner of *Pf*Kelch13: To study the transgenic A549 (*Pf*Kelch13-GFP) proteins and their interacting partners, we used immunoprecipitation (IP) that utilises the GFP affinity matrix or specific antibodies. Since previous experiments suggest that the *Pf*Kelch13 functions similarly to KEAP1 under oxidative stress and thus interactions of *Pf*Kelch13 proteins with Nrf2 were the only possibility for *Pf*Kelch13 to function similarly to Keap1. Equal volumes of the total extracts from transgenic *Pf*Kelch13-GFP cells and AcGFP cells (used as a control) after their overnight incubation with anti-GFP coupled beads were taken. Now, half of the fraction of these protein-incubated GFP antibody coupled beads was used in the western blot probed with anti-GFP antibody.

The band observed was approximately 110 kDa (Figure 8A) in the transgenic *Pf*Kelch13-GFP protein sample loaded lane of the SDS gel, while it was approximately 27 kDa band (Figure 8A) in the transgenic AcGFP (control) protein sample loaded lane of the SDS gel. That confirms the binding of *Pf*Kelch13-GFP and AcGFP protein lysate with the GFP antibody coupled beads. We used the other half of the fraction of these protein incubated GFP antibody coupled beads in the western blot and probed it with anti-Nrf2 antibody and here we observed the band of approximately 110 kDa (Figure 8B) in transgenic *Pf*Kelch13-GFP protein sample loaded lane of the SDS gel while approximately no band of 110 kDa was observed in transgenic AcGFP (control) protein sample loaded lane of the SDS gel. Thus, Nrf2 was proved to be the interacting partner of *Pf*Kelch13.

Discussion

*Pf*Kelch13 is an essential protein that comprises of BTB and Kelch-repeat propeller (KREP) domains. These domains are commonly found in E3 ubiquitin ligase complexes that target substrate proteins for ubiquitin-dependent degradation[3,22,27]. *Pf*Kelch13 is thought to bind to substrate proteins; however, its functional role linking artemisinin resistance mutations is unknown. One of the other proteins known for a similar structure is the human protein known as Keap1, which also comprises of the BTB and Kelch-repeat propeller (KREP) domains. Keap1 is a substrate adaptor protein that interacts with Cul3 and Rbx1 to ubiquitinate and degrade Nrf2[6]. This approach inhibits the cellular response to oxidative stress. Thus, based on their evolutionary background, KLHL family members have been speculated as human orthologs of *Pf*Kelch13, but no studies have been done that conclude that *Pf*Kelch13's functional role is similar to Keap1[6].

Our goal here was to study the functional role of *Pf*Kelch13 in comparison to well-established reports on the Keap1 function. The crystal structures available for *Pf*Kelch13 only possess information on the BTB and KREP domains[11]. Using bioinformatics, we predicted the full-length structure of *Pf*Kelch13 with the AlphaFold3 server, showing that the KREP domain had the highest confidence level in prediction. Superimposing the *Pf*Kelch13 and Keap1 structures, we found an RMSD value of 3.33 and 22% identity for the predicted full-length structure and an RMSD value of 1.45 and 25% identity for the PDB database structure. In both cases, the amino acid sequences in the KREP domain region showed maximum structural similarity (Figure 4 D-E). The sequence alignment of the proteins was also checked using Clustal Omega (https://www.ebi.ac.uk/jdispatcher/msa/clustalo).

Results showed that most of the identical amino acids in both proteins were mainly located in the KREP domain regions. The KREP domain is the region known in Keap1 with most of the mutations (G333C, G350S, G364C, G379D, R413L, R415G, A427V, G430C, R470C, R470H, R470S and G476R) responsible for cancer as well as the region in *Pf*Kelch13 with most common mutations like C580Y and R539T that are known to confer artemisinin resistance[22]. This study revealed that *Pf*Kelch13 shows sequence similarity as well as structural similarity with the Keap1 and KREP domains of *Pf*Kelch13, which may have similar functional/interaction sites.

To assess the distribution of *Pf*Kelch13 in mammalian cells and to correlate it with the Keap1, we first decided to express *Pf*Kelch13 in the mammalian expression vector (pAcGFP1-C1) with the sequences expressing GFP at the C-terminus of the fusion protein. The presence of the GFP sequence helped to identify the successful transfection of *Pf*Kelch13 into the transfected mammalian cells in live cell imaging of A549, which was earlier established as low Keap1 expressing cells in the western blot (Figure 5A). It has been reported that A549 was a low Keap1-expressing cell line and the function of Keap1 was already known in previous studies. Accordingly, we designed our experiments according to the role of Keap1 to better understand how Keap1 acts as a functional homolog of *Pf*Kelch13.

Many studies explained and proved that the cellular localization of Keap1 was mostly in the cytoplasm of the mammalian cells under the basal condition and the

localization of Keap1 remains the same even under stress conditions. Moreover, we performed the IFA in transgenic A549 (*Pf*Kelch13-GFP) and (AcGFP) using an anti-GFP antibody, where AcGFP acted as a control. The results explained that the GFP signal was present in the cytoplasmic region of the cell i.e. the localization of *Pf*Kelch13-GFP was mostly in the cytoplasm of cells (A549), while the GFP signal due to GFP in AcGFP seemed to be more intense in the nucleus with weak and dispersed cytoplasmic signal, which suggested that the green fluorescence signal in the cytoplasmic region in transgenic A549 (*Pf*Kelch13-GFP) was not due to the only GFP but it was due to the localization of *Pf*Kelch13 protein in the cellular of A549 cells. Based on their localization profile, both *Pf*Kelch13 and Keap1 were similar. After looking at the localization profile similarity of *Pf*Kelch13 with Keap1, we compared it with the functional role of Keap1 as the study explained that Keap1 functions as a negative regulator of transcriptional factor Nrf2.

As reported, Keap1 undergoes structural changes under oxidative conditions, causing Nrf2 dissociation. The latter protein subsequently aggregates into the nucleus and forms a heterodimer with musculoaponeurotic fibrosarcoma (Maf), which combines with antioxidant response elements (AREs) to activate the transcription of numerous antioxidants[36].

So, we treated the transgenic A549 (*Pf*Kelch13-GFP and AcGFP) as well as non-transfected A549 under similar oxidative stress with different concentrations of H_2O_2 to induce oxidative stress and cellular injuries. We calculated an optimal concentration of H_2O_2 where there was oxidative stress without substantial cell death to study the effect of stress on the cells[30]. The effect of H_2O_2 on the cell viability of transgenic A549 (*Pf*Kelch13-GFP and AcGFP) as well as non-transfected A549 was measured first with the help of cell viability assay (MTT Assay). Results revealed a decrease in the cell viability of both the transgenic A549 (*Pf*Kelch13-GFP and AcGFP) as well as non-transfected A549 with the increased concentration of H_2O_2, but the rate at which the cell viability decreased in all the cells with the increasing concentration of H_2O_2, was different.

The rate at which the cell viability of transgenic A549 (*Pf*Kelch13-GFP) cells decreased was comparatively less than both transgenic A549 (AcGFP) and non-transfected A549. Thus, it suggested that *Pf*Kelch13 shows a similar defensive mechanism under the oxidative stress condition to protect the oxidative damage to the cells the way it was already known in the Keap1, which further strengthened the possibility of *Pf*Kelch13 acting similarly to the Keap1-Nrf2 system, as has been known as a key cellular defense mechanism. We planned our next experiment accordingly from the MTT assay data by selecting the exposure to 100 µM H_2O_2 to both the transgenic A549 (AcGFP) as well as non-transfected A549 control for 24 hours as the cell viability in both cells was found to be approximately 50%. After H_2O_2 exposure, the total RNA isolated, cDNA prepared and the relative levels of cryoprotective gene expression (*HO1, NQO1*) were evaluated by RT-qPCR (Figures 7 B and C).

Results revealed that levels of *HO1* and *NQO1* increased threefold in the presence of *Pf*Kelch13. We also found that *Pf*Kelch13 behaved similarly as the transgenic A549 (*Pf*Kelch13-GFP) mRNA expression of HO1 was significantly higher than both non-transfected A549 and in cells expressing AcGFP, *Pf*Kelch13 followed a similar defense mechanism under oxidative stress like Keap1. However, in the case of mRNA, the expression of *nqo1* in transgenic A549 (*Pf*Kelch13-GFP) was significantly higher than non-transfected A549 but lower in cells expressing AcGFP. Hence, we concluded that *Pf*Kelch13, under oxidative stress, follows a similar pathway to protect the cell as Keap1.

To investigate if *Pf*Kelch13 has a similar pathway to Keap1, we checked Nrf2 as a binding partner for *Pf*Kelch13 by coimmunoprecipitation. We took both transgenic *Pf*Kelch13-GFP and transgenic AcGFP (as control) cell lysates in equal volumes and checked their expression after overnight incubation with GFP antibody coupled beads with the help of western blot to confirm the binding of *Pf*Kelch13-GFP and AcGFP with the beads. Under similar conditions, we checked Nrf2 as an interacting partner of *Pf*Kelch13 through western blot using anti-Nrf2 and we found a band of 110 kDa in the blot in the *Pf*Kelch13-GFP lane, which matched the approximate molecular mass of Nrf2. There was no band of such size in the control (AcGFP).

Since Nrf2 acts as the interacting partner of *Pf*Kelch13, this study showed functional similarity between *Pf*Kelch13 and human Keap1, which implicates their functional conservation.

Conclusion

Both *Pf*Kelch13 and Keap1 proteins belong to the same family, as they both contain BTB and KREP. These domains are commonly found in E3 ubiquitin ligase complexes that target substrate proteins for ubiquitin-dependent degradation [3,15,22,27]. *Pf*Kelch13 is thought to bind to substrate proteins. However, its functional role linking artemisinin resistance mutations is unknown. Keap1 is a substrate adaptor protein that interacts with Cul3 and Rbx1 to ubiquitinate and degrade Nrf2[15].

Our goal was to study the functional role of *Pf*Kelch13 in comparison to Keap1. Using bioinformatics, we predicted the full-length structure of *Pf*Kelch13 with the AlphaFold3 server, showing that the KREP domain had the highest confidence level in prediction. Superimposing the *Pf*Kelch13 and Keap1, Alphafold3 predicted structures as well as the *Pf*Kelch13 and Keap1 PDB database structure. In both cases, the amino acid sequences in the KREP domain region showed maximum structural similarity and most of the identical amino acids in both proteins were mainly located in the KREP domain regions.

To assess the distribution of *Pf*Kelch13 in mammalian cells and to correlate it with Keap1, we decided to express *Pf*Kelch13 in the mammalian expression vector (pAcGFP1-C1) with the sequences expressing GFP at the C-terminus of the fusion protein. We performed the IFA in transgenic A549 (*Pf*Kelch13-GFP) and (AcGFP). The results explained that the GFP signal was present in the cytoplasmic region of the cell i.e. the localization of *Pf*Kelch13-GFP was mostly in the cytoplasm of cells (A549), while the GFP signal due to GFP seemed to be more intense in the nucleus with weak and dispersed cytoplasmic signal, which suggested that the green fluorescence signal in the cytoplasmic region in transgenic A549 (*Pf*Kelch13-GFP) was not due to the only GFP but it was due to the localization of *Pf*Kelch13 protein. This proved that based on their localization profile, both *Pf*Kelch13 and Keap1 were similar.

After looking at the localization profile similarity of *Pf*Kelch13 with Keap1, we compared it with the functional role of Keap1 as the study explained that Keap1 functions as a negative regulator of transcriptional factor Nrf2. The transgenic A549 (*Pf*Kelch13-GFP and AcGFP) and non-transfected A549 were treated under similar oxidative stress with different concentrations of H_2O_2 to induce oxidative stress and cellular injuries. Results revealed a decrease in the cell viability of both the transgenic A549 (*Pf*Kelch13-GFP and AcGFP) as well as non-transfected A549 with the increased concentration of H_2O_2. The rate at which the cell viability of transgenic A549 (*Pf*Kelch13-GFP) cells decreased was comparatively less than both transgenic A549 (AcGFP) and non-transfected A549.

Thus, it suggested that *Pf*Kelch13 shows a similar defensive mechanism under the oxidative stress condition to protect the oxidative damage to the cells the way it was already known in the Keap1, which further strengthened the possibility of *Pf*Kelch13 acting similarly to the Keap1-Nrf2 system. Our RT-qPCR results revealed that levels of HO1 and NQO1 increased threefold in the presence of *Pf*Kelch13. We also found that *Pf*Kelch13 behaved similarly as the transgenic A549 (*Pf*Kelch13-GFP) mRNA expression of HO1 was significantly higher than both non-transfected A549 and in cells expressing AcGFP, which suggested that *Pf*Kelch13 followed a similar defense mechanism under oxidative stress like Keap1. However, in the case of mRNA expression of NQO1 in transgenic A549 (*Pf*Kelch13-GFP), it was significantly higher than non-transfected A549 but lower in cells expressing AcGFP.

To investigate if *Pf*Kelch13 has a similar pathway to Keap1, we checked Nrf2 as a binding partner for *Pf*Kelch13 by coimmunoprecipitation. Under similar conditions, we checked Nrf2 as an interacting partner of *Pf*Kelch13 through western blot using anti-Nrf2 and we found a band of 110 kDa band in the blot in *Pf*Kelch13-GFP lane, which matched the approximate molecular mass of Nrf2. There was no band of such size in the control (AcGFP). Since Nrf2 acts as the interacting partner of *Pf*Kelch13, this study showed functional similarity between *Pf*Kelch13 and human Keap1, which implicates their functional conservation.

Acknowledgement

The author would like to thank her Ph.D. supervisor, Dr. Souvik Bhattacharjee, Special Centre for Molecular Medicine, for the conception of the idea and experimental design and for providing laboratory infrastructure and reagents during this study. The author also thanks Prof. Vibha Tandon from the Special Centre for Molecular Medicine, JNU and Dr Dinkar Sahal from ICGEB for providing the mammalian cell lines. NP is a recipient of a research fellowship (MANF-2018-19-UTT-100044) from the University Grants Commission, Maulana Azad National Fellowship, Government of India.

References

1. Ashley E.A., Dhorda M., Fairhurst R.M., Amaratunga C., Lim P., Suon S., Sreng S., Anderson J.M., Mao S., Sam B., Sopha C., Chuor C.M., Nguon C., Sovannaroth S., Pukrittayakamee S., Jittamala P., Chotivanich K., Chutasmit K., Suchatsoonthorn C., Runcharoen R., Hien T.T., Thuy-Nhien N.T., Thanh N.V., Phu N.H., Htut Y., Han K.T., Aye K.H., Mokuolu O.A., Olaosebikan R.R., Folaranmi O.O., Mayxay M., Khanthavong M., Hongvanthong B., Newton P.N., Onyamboko M.A., Fanello C.I., Tshefu A.K., Mishra N., Valecha N., Phyo A.P., Nosten F., Yi P., Tripura R., Borrmann S., Bashraheil M., Peshu J., Faiz M.A., Ghose A., Hossain M.A., Samad R., Rahman M.R., Hasan M.M., Islam A., Miotto O., Amato R., MacInnis B., Stalker J., Kwiatkowski D.P., Bozdech Z., Jeeyapant A., Cheah P.Y., Sakulthaew T., Chalk J., Intharabut B., Silamut K., Lee S.J., Vihokhern B., Kunasol C., Imwong M., Tarning J., Taylor W.J., Yeung S., Woodrow C.J., Flegg J.A., Das D., Smith J., Venkatesan M., Plowe C.V., Stepniewska K., Guerin P.J., Dondorp A.M., Day N.P. and White N.J., Spread of Artemisinin Resistance in *Plasmodium falciparum* Malaria, *New England Journal of Medicine*, **371**, 411–423 **(2014)**

2. Birnbaum J., Scharf S., Schmidt S., Jonscher E., Anna W., Hoeijmakers M., Flemming S., Geeke Toenhake C., Schmitt M., Sabitzki R., Bergmann B., Fröhlke U., Mesén-Ramírez P., Soares A.B., Herrmann H., Bártfai R. and Spielmann T., A Kelch13-defined endocytosis pathway mediates artemisinin resistance in malaria parasites, *Science*, **367(6473)**, 51-59 **(2020)**

3. Canning P., Cooper C.D.O., Krojer T., Murray J.W., Pike A.C.W., Chaikuad A., Keates T., Thangaratnarajah C., Hojzan V., Marsden B.D., Gileadi O., Knapp S., Von Delft F. and Bullock A.N., Structural basis for Cul3 protein assembly with the BTB-Kelch family of E3 ubiquitin ligases, *Journal of Biological Chemistry*, **288**, 7803–7814 **(2013)**

4. Changjiang L., Cheng L., Haitao W., Peijie H., Zhang Y., Yang Y., Chen J. and Chen M., Activation of the KEAP1-NRF2-ARE signaling pathway reduces oxidative stress in Hep2 cells, *Mol Med* Rep., **18(3)**, 2541–2550 **(2018)**

5. Cleasby A., Yon J., Day P.J., Richardson C., Tickle I.J., Williams P.A., Callahan J.F., Carr R., Concha N., Kerns J.K., Qi H., Sweitzer T., Ward P. and Davies T.G., Structure of the BTB domain of Keap1 and its interaction with the triterpenoid antagonist CDDO, *PLoS One*, **9(6)**, e98896 **(2014)**

6. Coppée R., Jeffares D.C., Miteva M.A., Sabbagh A. and Clain J., Comparative structural and evolutionary analyses predict functional sites in the artemisinin resistance malaria protein K13, *Sci Rep*, **9**, 10675 **(2019)**

7. Cullinan S.B., Gordan J.D., Jin J., Harper J.W. and Diehl J.A., The Keap1-BTB Protein Is an Adaptor That Bridges Nrf2 to a Cul3-Based E3 Ligase: Oxidative Stress Sensing by a Cul3-Keap1 Ligase, *Mol Cell Biol*., **24(19)**, 8477–8486 **(2004)**

8. Deshmukh P., Unni S., Krishnappa G. and Padmanabhan B., The Keap1–Nrf2 pathway: promising therapeutic target to counteract ROS-mediated damage in cancers and neurodegenerative diseases, *Biophys Rev*., **9(1)**, 41-56 **(2017)**

9. Dhakshinamoorthy S. and Jaiswal A., Functional characterization and role of INrf2 in antioxidant response element-mediated expression and antioxidant induction of NAD(P)H: quinone oxidoreductase1 gene, *Oncogene*, **20(29)**, 3906–3917 **(2001)**

10. Dhanoa B.S., Cogliati T., Satish A.G., Bruford E.A. and Friedman J.S., Update on the Kelch-like (KLHL) gene family, *Hum Genomics*, **7(1)**, 13 **(2013)**

11. Goel N., Dhiman K., Kalidas N., Mukhopadhyay A., Ashish F. and Bhattacharjee S., *Plasmodium falciparum* Kelch13 and its artemisinin-resistant mutants assemble as hexamers in solution: a SAXS data-driven modelling study, *FEBS Journal*, **289(16)**, 4935–4962 **(2022)**

12. Harald Noedl M.D. et al, Evidence of Artemisinin-Resistant Malaria in Western Cambodia, *N Engl J Med.*, **359(24)**, 2619-20 **(2008)**

13. He J., Zhang X., Lian C., Wu J., Fang Y. and Ye X., KEAP1/NRF2 axis regulates H_2O_2-induced apoptosis of pancreatic β-cells, *Gene*, **691**, 8–17 **(2019)**

14. Itoh K., Wakabayashi N., Katoh Y., Ishii T., Igarashi K., Douglas Engel J. and Yamamoto M., Keap1 represses nuclear activation of antioxidant responsive elements by Nrf2 through binding to the amino-terminal Neh2 domain, *Genes*, **13(1)**, 76-86 **(1999)**

15. Kansanen E., Kuosmanen S.M., Leinonen H. and Levonenn A.L., The Keap1-Nrf2 pathway: Mechanisms of activation and dysregulation in cancer, *Redox Biol*., **1(1)**, 45-9 **(2013)**

16. Kaspar J.W., Niture S.K. and Jaiswal A.K., Nrf2:INrf2 (Keap1) signaling in oxidative stress, *Free Radic Biol Med*., **47(9)**, 1304-9 **(2009)**

17. Katoh Y., Iida K., Kang M. Il, Kobayashi A., Mizukami M., Tong K.I., McMahon M., Hayes J.D., Itoh K. and Yamamoto M., Evolutionary conserved N-terminal domain of Nrf2 is essential for the Keap1-mediated degradation of the protein by proteasome, *Archives of Biochemistry and Biophysics*, **433(2)**, 342–350 **(2005)**

18. Kobayashi A., Kang M.I., Okawa H., Ohtsuji M., Zenke Y., Chiba T., Igarashi K. and Yamamoto M., Oxidative Stress Sensor Keap1 Functions as an Adaptor for Cul3-Based E3 Ligase To Regulate Proteasomal Degradation of Nrf2, *Mol Cell Biol*., **24**, 7130–7139 **(2004)**

19. Kobayashi A., Kang M.I., Watai Y., Tong K.I., Shibata T., Uchida K. and Yamamoto M., Oxidative and Electrophilic Stresses Activate Nrf2 through Inhibition of Ubiquitination Activity of Keap1, *Mol Cell Biol*., **26**, 221–229 **(2006)**

20. Kobayashi M., Itoh K., Suzuki T., Osanai H., Nishikawa K., Katoh Y., Takagi Y. and Yamamoto M., Identification of the interactive interface and phylogenic conservation of the Nrf2-Keap1 system, *Genes to Cells*, **7**, 807–820 **(2002)**

21. Maïga-Ascofaré O. and May J., Is the A578S single-nucleotide polymorphism in K13-propeller a marker of emerging resistance to artemisinin among *Plasmodium falciparum* in Africa?, *Journal of Infectious Diseases*, **213(1)**, 165–166 **(2016)**

22. Martinez V.D., Vucic E.A., Thu K.L., Pikor L.A., Lam S. and Lam W.L., Disruption of KEAP1/CUL3/RBX1 E3-ubiquitin ligase complex components by multiple genetic mechanisms: Association with poor prognosis in head and neck cancer, *Head Neck*, **37**, 727–734 **(2015)**

23. Motohashi H. and Yamamoto M., Nrf2-Keap1 defines a physiologically important stress response mechanism, *Trends Mol Med*., **10(11)**, 549-57 **(2004)**

24. Padmanabhan B., Tong K.I., Ohta T., Nakamura Y., Scharlock M., Ohtsuji M., Kang M. Il, Kobayashi A., Yokoyama S. and Yamamoto M., Structural basis for defects of Keap1 activity provoked by its point mutations in lung cancer, *Mol Cell*, **21**, 689–700 **(2006)**

25. Prag S. and Adams J.C., Molecular phylogeny of the kelch-repeat superfamily reveals an expansion of BTB/kelch proteins in animals, *BMC Bioinformatics*, doi: 10.1186/1471-2105-4-42 **(2003)**

26. Probst B.L., McCauley L., Trevino I., Wigley W.C. and Ferguson D.A., Cancer cell growth is differentially affected by constitutive activation of NRF2 by KEAP1 deletion and pharmacological activation of NRF2 by the synthetic triterpenoid, RTA 405, *PLoS One*, **10(8)**, e0135257 **(2015)**

27. Shi X., Xiang S., Cao J., Zhu H., Yang B., He Q. and Ying M., Kelch-like proteins: Physiological functions and relationships with diseases, *Pharmacol Res*., **148**, 104404 **(2019)**

28. Singh A., Misra V., Thimmulappa R.K., Lee H., Ames S., Hoque M.O., Herman J.G., Baylin S.B., Sidransky D., Gabrielson E., Brock M.V. and Biswal S., Dysfunctional KEAP1-NRF2 interaction in non-small, *PLoS Med*., **3(10)**, e420 **(2006)**

29. Stogios P.J. and Privé G.G., Protein Sequence Motif The BACK domain in BTB-kelch proteins, *Update TRENDS in Biochemical Sciences*, **29(12)**, 634-7 **(2004)**

30. Tan J., Li P., Xue H. and Li Q., Cyanidin-3-glucoside prevents hydrogen peroxide (H2O2)-induced oxidative damage in HepG2 cells, *Biotechnol Lett*., **42(11)**, 2453–2466 **(2020)**

31. Tong K.I., Padmanabhan B., Kobayashi A., Shang C., Hirotsu Y., Yokoyama S. and Yamamoto M., Different Electrostatic Potentials Define ETGE and DLG Motifs as Hinge and Latch in Oxidative Stress Response, *Mol Cell Biol*., **27(21)**, 7511–7521 **(2007)**

32. Uruno A. and Motohashi H., The Keap1-Nrf2 system as an *in vivo* sensor for electrophiles, *Nitric Oxide - Biology and Chemistry*, **25(2)**, 153–160 **(2011)**

33. Venkatesan P., The 2023 WHO World Malaria Report, *Lancet Microbe*, **5**, e214 **(2024)**

34. Wakabayashi N., Dinkova-Kostova A.T., David Holtzclaw W., Kang M.I., Kobayashi A., Yamamoto M., Kensler T.W. and Talalay P., Protection against electrophile and oxidant stress by induction of the phase 2 response: Fate of cysteines of the Keap1 sensor modified by inducers, *Proc Natl Acad*, **101(7)**, 2040-5 **(2003)**

35. Wakabayashi N., Itoh K., Wakabayashi J., Motohashi H., Noda S., Takahashi S., Imakado S., Kotsuji T., Otsuka F., Roop D.R., Harada T., Engel J.D. and Yamamoto M., Keap1-null mutation leads to postnatal lethality due to constitutive Nrf2 activation, *Nat Genet.*, **35(3)**, 238–245 **(2003)**

36. Wilson C.J., Chang M., Karttunen M. and Choy W.Y., Keap1 cancer mutants: A large-scale molecular dynamics study of protein stability, *Int J Mol Sci*., **22(10)**, 5408 **(2021)**

37. Witkowski B., Amaratunga C., Khim N., Sreng S., Chim P., Kim S., Lim P., Mao S., Sopha C., Sam B., Anderson J.M., Duong S., Chuor C.M., Taylor W.R.J., Suon S., Mercereau-Puijalon O., Fairhurst R.M. and Menard D., Novel phenotypic assays for the detection of artemisinin-resistant *Plasmodium falciparum* malaria in Cambodia: *In-vitro* and ex-vivo drug-response studies, *Lancet Infect Dis*., **13**, 1043–1049 **(2013)**

38. Ye G., Wang J., Yang W., Li J., Ye M. and Jin X., The roles of KLHL family members in human cancers, *Am J Cancer Res.*, **12(11)**, 5105-5139 **(2022)**

39. Yu C. and Xiao J.H., The Keap1-Nrf2 System: A Mediator between Oxidative Stress and Aging, Oxid *Med Cell Longev*., **2021**, 16 **(2021)**

40. Zhang D.D. and Hannink M., Distinct Cysteine Residues in Keap1 Are Required for Keap1-Dependent Ubiquitination of Nrf2 and for Stabilization of Nrf2 by Chemopreventive Agents and Oxidative Stress, *Mol Cell Biol*., **23**, 8137–8151 **(2003)**

41. Zhang D.D., Lo S.C., Cross J.V., Templeton D.J. and Hannink M., Keap1 Is a Redox-Regulated Substrate Adaptor Protein for a Cul3-Dependent Ubiquitin Ligase Complex, *Mol Cell Biol*., **24(24)**, 10941–10953 **(2004)**.

(Received 18th November 2024, accepted 29th January 2025)